Electronic structure of an organic/metal interface: Pentacene/Cu(110)

Kathrin Müller,[†,‖] Ari P Seitsonen,[‡] Thomas Brugger,[¶] James Westover,[§] Thomas Greber,[¶] Thomas Jung,[†] and Abdelkader Kara[*,§]

Laboratory for Micro- and Nanotechnology, Paul Scherrer Institut, CH-5232 Villigen PSI, Switzerland, Physikalisch-Chemisches Institut, University of Zurich, Winterthurerstrasse 190, CH-8057 Zurich, Switzerland, Physik-Institut, University of Zurich, CH-8057 Zürich, Switzerland, and Department of Physics, University of Central Florida, Orlando FL 32816, USA

E-mail: Abdelkader.Kara@ucf.edu

---

[*]To whom correspondence should be addressed

[†]Laboratory for Micro- and Nanotechnology, Paul Scherrer Institut, CH-5232 Villigen PSI, Switzerland

[‡]Physikalisch-Chemisches Institut, University of Zurich, Winterthurerstrasse 190, CH-8057 Zurich, Switzerland

[¶]Physik-Institut, University of Zurich, CH-8057 Zürich, Switzerland

[§]Department of Physics, University of Central Florida, Orlando FL 32816, USA

[‖]Present address: Zernike Institute for Advanced Materials, University of Groningen, Nijenborgh 4, NL-9747 AG Groningen, Netherlands

Molecular orbitals and symmetry of pentacene molecule
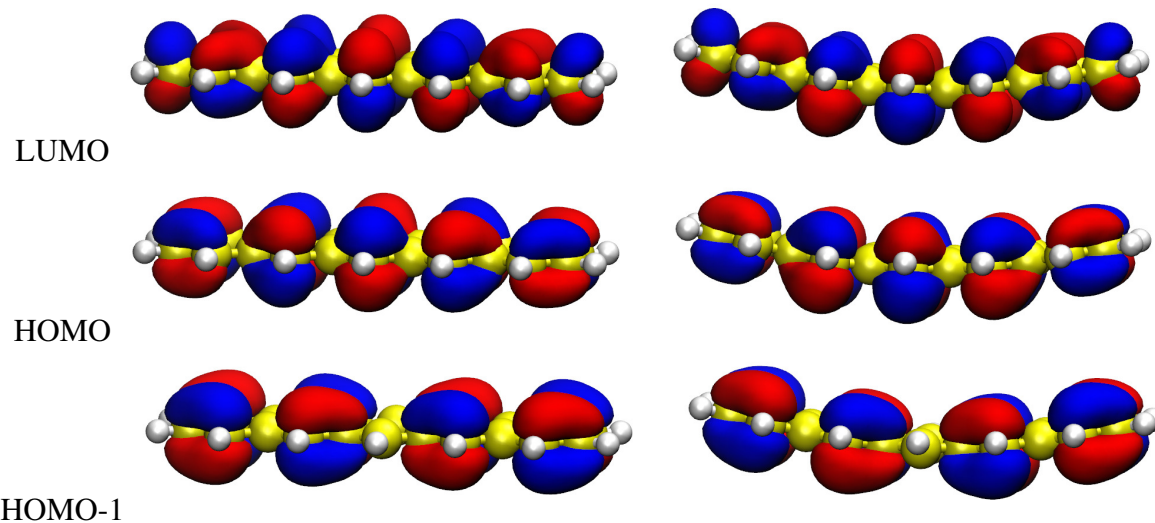

LUMO

HOMO

HOMO-1

Figure 1: a) Molecular orbitals of pentacene. Left: Gas phase structure, right: geometry extracted from pc/Cu(110).

The free pentacene molecule has the point group D_{2h}, whose character table is reproduced in Table 1.

Table 1

	E	$C_2\ (z)$	$C_2\ (y)$	$C_2\ (z)$	i	$\sigma\ (xy)$	$\sigma\ (xz)$	$\sigma\ (yz)$	linear, rotations	quadratic
A_g	1	1	1	1	1	1	1	1		x^2, y^2, z^2
B_{1g}	1	1	-1	-1	1	1	-1	-1	R_z	xy
B_{2g}	1	-1	1	-1	1	-1	1	-1	R_y	xz
B_{3g}	1	-1	-1	1	1	-1	-1	1	R_x	yz
A_u	1	1	1	1	-1	-1	-1	-1		
B_{1u}	1	1	-1	-1	-1	-1	1	1	z	
B_{2u}	1	-1	1	-1	-1	1	-1	1	y	
B_{3u}	1	-1	-1	1	-1	1	1	-1	x	

Further analysis from DFT calculations

We present here some additional results from the density functional theory (DFT) calculations that clarifies the convergence of the results with respect to the size of the slab model for the

substrate used, and results from a DFT exchange-correlation functional that does not contain the van der Waals interactions. We also analyse more in detail the bonding mechanism of the hybridisation of the states of the substrate with the pentacene molecule.

– vdW-DF functional in 8-layer slab

We have extended the four-layer slab used in the analysis of the main article by adding four atomic layers of the substrate at bulk-truncated positions. No atomic relaxation is performed.

Figure 2 contains the same analysis of the density difference as in the main article. The differences between the four- and eight-layer slabs is small.

Likewise the orbital overlap, $\mathscr{O}(E)$, in Figure 3 is very similar to the case of four layers, shown in the main article. Here we also show the projection on orbital LUMO+1: This orbital does not undergo any significant splitting.

– GGA functional

These results were calculated using four layers of substrate, like with the vdW-DF results in the main article.

The orbital overlap, $\mathscr{O}(E)$, in Figure 4 is similar to the one calculated with the vdW-DF. We notice, however, that the HOMO-1, HOMO and LUMO levels are deeper in energy, and the hybridisation splitting is larger there.

Furthermore, we have calculated the orbital overlap in geometries obtained by lifting the pentacene molecule rigidly away from the optimised geometry by an amount Δz. These results are shown in Figure 5. The curves show the broadening and splitting of bands when the molecule approaches the surface, and that at large separation the occupied (in particular HOMO) and unoccupied (LUMO) align so that the molecule remains practically neutral even if the Fermi level of Cu(110) is aligned with the molecule.
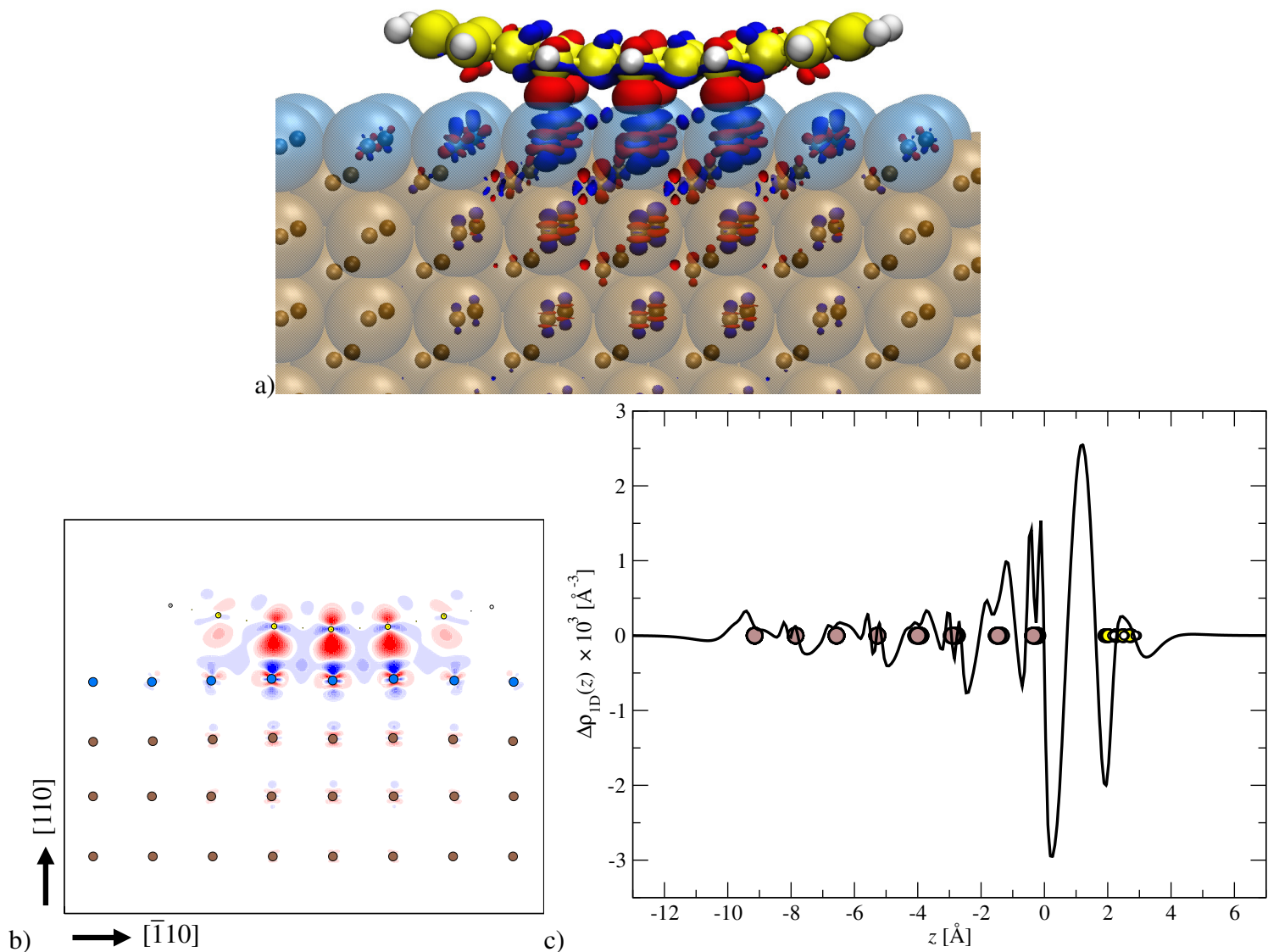
3

Figure 2: Difference in charge density upon adsorption of pentacene on Cu(110) from the calculations with vdW-DF functional in an 8-layer slab. a) Three-dimensional representation; the blue regions correspond to increased charge density, or decreased electron density, and the red regions to decreased charge density or increased electron density. b) A cut of the density different in the plane containing the surface normal and passing through the carbon atom C10. The atoms near to this plane have been marked with filled circles. c) The density difference averaged over the planes parallel to the surface.
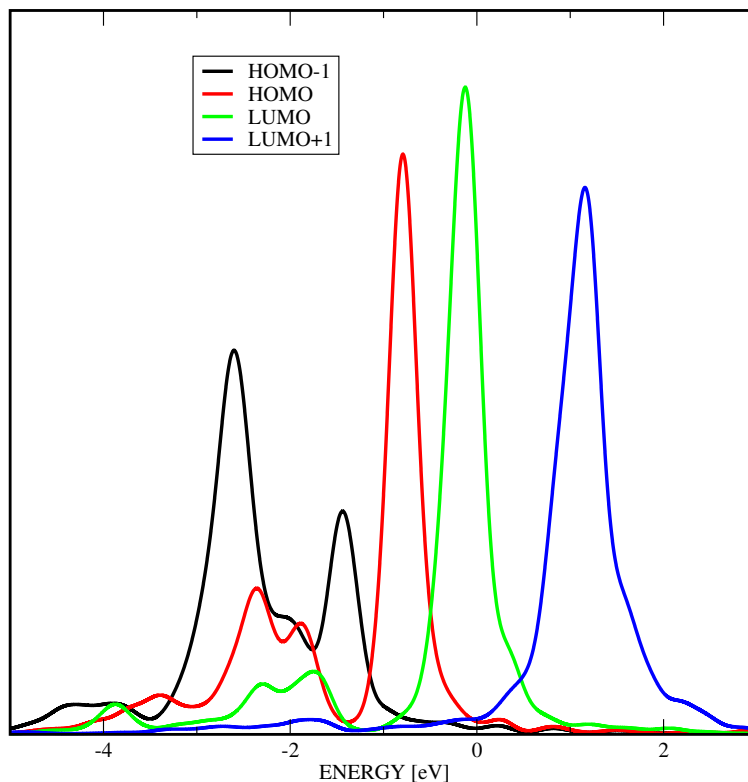
Figure 3: Projection of the Kohn-Sham states on the molecular orbitals, or the orbital overlap $\mathscr{O}(E)$, using the vdW-DF functional in an 8-layer slab.

Figure 5 also includes the eigenvalues of the frontier orbitals of the bent pentacene molecule in the optimised adsorption geometry and the optimised molecule in the gas phase. The HOMO levels were aligned to the value of the molecule lifted by 2.5 Å from the surface. We see that the separation of the eigenvalues does not change when the substrate is removed, but the unoccupied LUMO and LUMO+1 orbitals are at relatively higher energies when in the gas phase molecule, that is when the molecule is allowed to relax and does no longer interact with its periodic images, where the influence due to the latter effect is small. This difference changes the gap between the occupied and unoccupied states, and thus the HOMO-LUMO gap, by 0.35 eV.
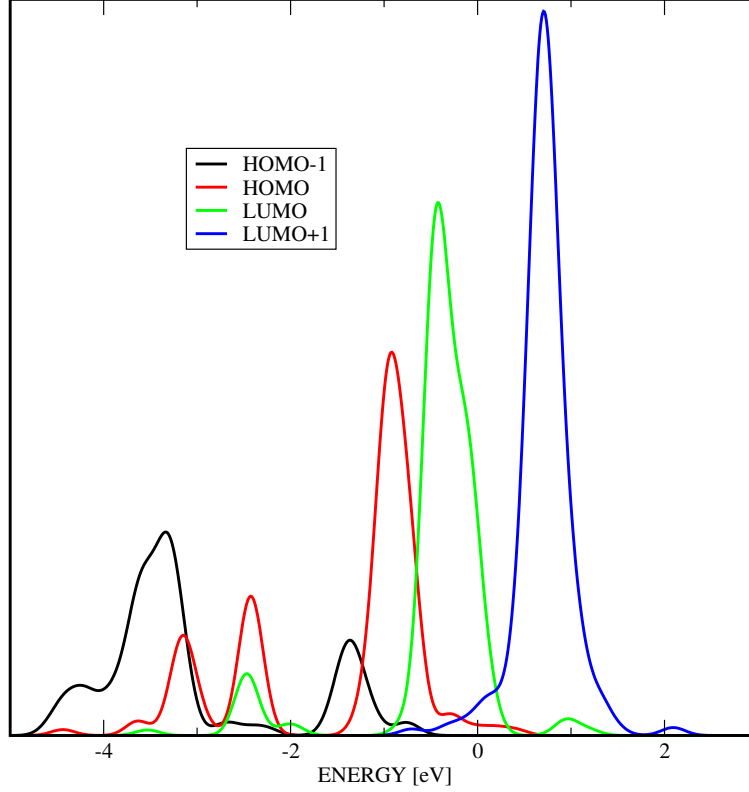
Figure 4: Projection of the Kohn-Sham states on the molecular orbitals, or the orbital overlap $\mathscr{O}(E)$, using the GGA-PBE functional.

– Hybridisation of substrate orbitals with pentacene

In order to understand better the hybridisation at the organic/metal interface we study the character of the orbital overlap times the projected density of states, $\mathscr{P}_{\text{Cu}}(E;lm)$, on the Cu atom beneath the C10,

$$\mathscr{O}(E) \times \mathscr{P}_{\text{Cu}}(E;lm) = \left|\langle\chi_j \mid \psi_{i\vec{k}}\rangle\right|^2 \left|\langle\phi_{\text{Cu}} \mid \psi_{i\vec{k}}\rangle\right|^2 \delta(E - E_{i\vec{k}}) \,,$$

where χ_j is the jth molecular orbital, $\psi_{i\vec{k}}$ the Kohn-Sham orbital $i\vec{k}$ and $\varepsilon_{i\vec{k}}$ the corresponding eigenvalue, and ϕ_{Cu} the atomic orbitals of the specific Cu atom. This product gives the largest contribution at the Cu orbitals that interact or hybridise strongest with the orbitals of pentacene.

In Figure 6 we see the result of this analysis. The peaks at the HOMO- and LUMO-derived

6

states arise mainly from the Cu-d_{xz} at the lower and Cu-d_{z^2} at the main peak, whereas several different d states of the Cu overlap with HOMO-1. This is because the HOMO-1 molecular orbital has a nodal plane above this Cu atom, thus making Cu-d_{z^2} an unfavourable orbital to interact with. At the other Cu atoms in the surface layer, above which the HOMO-1 does not have a nodal plane, the hybridisation again arises mainly from the Cu-d_{z^2}.
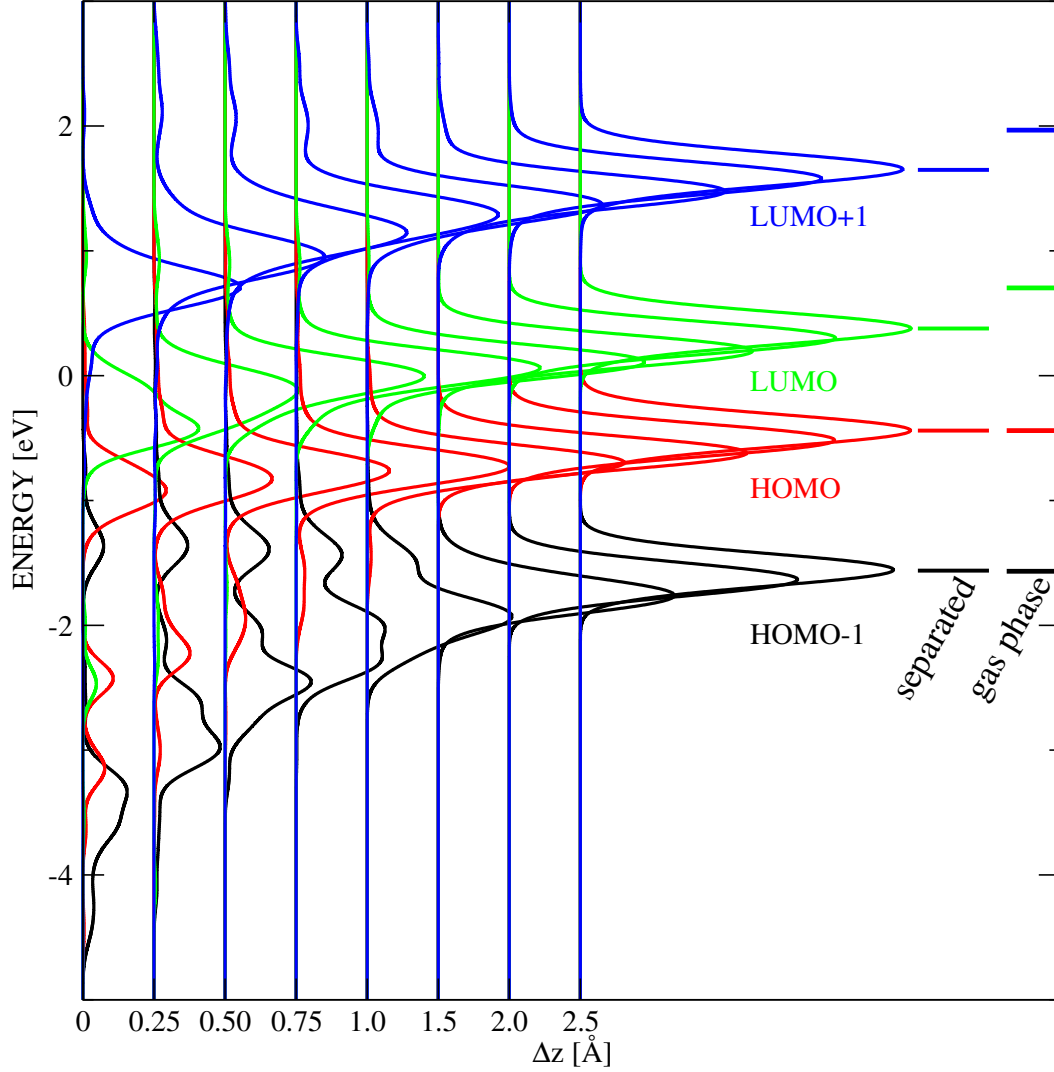
Figure 5: Projection of the Kohn-Sham states on the molecular orbitals, or the orbital overlap $\mathcal{O}(E)$, upon lifting the pentacene molecule rigidly away from the substrate, using the GGA-PBE functional. The eigenvalues of the molecule far away, "separated", and a free, relaxed molecule, "gas phase", are indicated as well.
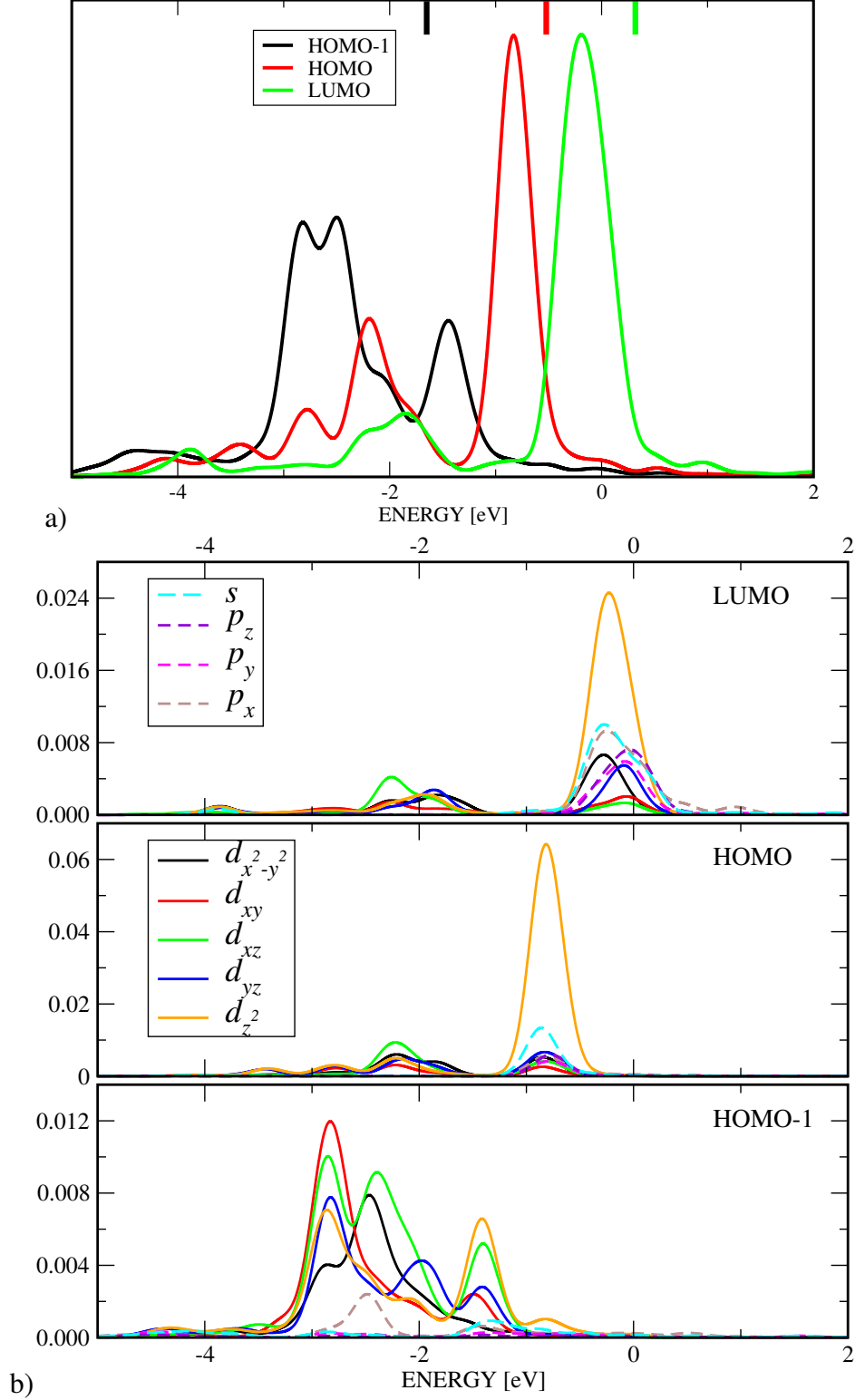
Figure 6: a) Orbital overlap $\mathcal{O}(E)$. The short vertical lines below to top axis denote the eigenvalues of the corresponding orbitals when the substrate is removed. b) Orbital overlap times the projected density of states $\mathcal{P}_{\text{Cu}}(E;lm)$ on the Cu atom beneath the C10, $\mathcal{O}(E) \times \mathcal{P}_{\text{Cu}}(E;lm)$. Four layers of substrate with the vdW-DF functional were employed.